RESEARCH

Possible association of dose rate and the development of late visual toxicity for patients with intracranial tumours treated with pencil beam scanned proton therapy

Arturs Meijers[1*], Juliane Daartz[2], Antje-Christin Knopf[3,4], Michelle van Heerden[1], Nicola Bizzocchi[1], Miriam Varela Vazquez[1], Barbara Bachtiary[1], Alessia Pica[1], Helen A Shih[5] and Damien Charles Weber[1,6,7]

Abstract

Background and purpose Rare but severe toxicities of the optic apparatus have been observed after treatment of intracranial tumours with proton therapy. Some adverse events have occurred at unusually low dose levels and are thus difficult to understand considering dose metrics only. When transitioning from double scattering to pencil beam scanning, little consideration was given to increased dose rates observed with the latter delivery paradigm. We explored if dose rate related metrics could provide additional predicting factors for the development of late visual toxicities.

Materials and methods Radiation-induced intracranial visual pathway lesions were delineated on MRI for all index cases. Voxel-wise maximum dose rate (MDR) was calculated for 2 patients with observed optic nerve toxicities (CTCAE grade 3 and 4), and 6 similar control cases. Additionally, linear energy transfer (LET) related dose enhancing metrics were investigated.

Results For the index cases, which developed toxicities at low dose levels (mean, 50 Gy_{RBE}), some dose was delivered at higher instantaneous dose rates. While optic structures of non-toxicity cases were exposed to dose rates of up to 1 to 3.2 Gy_{RBE}/s, the pre-chiasmatic optic nerves of the 2 toxicity cases were exposed to dose rates above 3.7 Gy_{RBE}/s. LET-related metrics were not substantially different between the index and non-toxicity cases.

Conclusions Our observations reveal large variations in instantaneous dose rates experienced by different volumes within our patient cohort, even when considering the same indications and beam arrangement. High dose rate regions are spatially overlapping with the radiation induced toxicity areas in the follow up images. At this point, it is not feasible to establish causality between exposure to high dose rates and the development of late optic apparatus toxicities due to the low incidence of injury.

Keywords Proton therapy, Dose rate, Visual toxicity, Radiation induced neuropathy

*Correspondence:
Arturs Meijers
arturs.meijers@psi.ch

Introduction

Proton therapy is a form of radiotherapy, that uses protons as a source of ionizing radiation [1]. Proton therapy was originally introduced through passively scattered delivery techniques (also known as single and double scattering modalities). In passively scattered modes the entire target volume is exposed to the proton beam multiple times per second. In the late 1990´s, the actively scanned proton beam modality was proposed and developed at Paul Scherrer Institut (PSI) [2]. Due to the laterally scattered and longitudinally modulated beam, the instantaneous dose rates in passively scattered modalities are considerably lower compared to those in the actively scanned modalities. Over the last decade, a rapid switch from passively scattered modalities to actively scanned ones has occurred worldwide [3]. In this transition, no extensive consideration was given to the change in instantaneous dose rates during proton irradiation.

Depending on the range of variation, the dose rate (DR) is known to influence radiobiological effectiveness and radiochemical processes [4–6]. The investigation of DR effects in external beam therapy, including proton therapy, is still limited. However, there is evidence suggesting a potential correlation between DR and relative biological effectiveness (RBE) in conventional photon beams [7–10]. In contrast, such effects have not been identified in carbon ion beams. Noteworthy, very limited data is available on DR effects in proton beams.

Rare, unexpected severe toxicities can occur in patients following proton therapy [11, 12]. A dedicated workshop on these remarkable toxicities was organized by the European Particle Therapy Network in 2022 (https://www.estro.org/Science/EPTN). Some of these reported toxicities occur at relatively low dose levels compared to the dose constraints applied in conventional photon therapy. Therefore, such events are rather unexpected and difficult to explain with a dose-metric paradigm. At PSI, we have observed rare but high-grade visual toxicity in elderly patients with or without hypertension and diabetes [12].

With regards to RBE of proton therapy, a constant factor of 1.1 is generally applied in clinical practice. However, evidence is mounting that RBE along the proton track is variable [13]. In most variable RBE models dose-averaged LET (LET_d), cell type and fractionation are considered. The available literature provides conflicting evidence regarding the relationship between elevated LET_d distributions and the occurrence of late toxicities.

It is our speculation that DR, along with other factors, may contribute to variations in relative biological effectiveness. In this preliminary study, we explore DR related metrics in an attempt to define additional parameters that may be predictive of optic apparatus toxicities. Such investigation was previously suggested by Daartz et al. [14].

Materials and methods

A selected number of treatment plans for patients with and without visual toxicity was analysed retrospectively. Toxicities to the intracranial visual pathways of these patients were identified during weekly follow-up meetings organized by the Study and Research Office within our department. Radiation induced optic neuropathy (RION) regions were identified on follow up MRI scans as a T1 contrast-enhancement of pre-chiasmatic optic nerve segments and contoured by a radiation oncologist (MD), in the absence of tumour progression. Matched control cases were chosen to represent a similar indication, within a similar tumour location treated at the same time period in the proximity of the optic apparatus as for the index cases with visual toxicities. No case with a follow-up period less than 10 months was considered in the evaluation. As reported in literature the expected development of optic toxicity post-irradiation is 10 to 20 months [15]. The characteristics of the selected cases are shown in Table 1.

Treatment plans were recalculated using an open-source Monte Carlo (MC) dose calculation engine MCsquare [16]. Every spot in the plan was calculated individually to obtain a set of spot-wise dose distributions. Each spot was simulated with 10^5 particles. Dose

Table 1 Summary of patient characteristics. Cases are labelled using nomenclature Tx-yy, where Tx indicates the grade of developed visual toxicity and yy indicates the number in the group

Patient	Diagnosis	I/C*	Sex	Age	Pr. dose**, Gy$_{RBE}$	Fx dose, Gy$_{RBE}$	Toxicity grade
T0-01	Meningioma, WHO Grade 2	C	F	47	55.8	1.8	0
T0-02	Meningioma, WHO Grade 1	C	F	59	50.4	1.8	0
T4-03	Mature Teratoma	I	M	34	50.4	1.8	4
T0-04	Meningioma, unspecified	C	F	47	50.4	1.8	0
T0-05	Meningioma, WHO Grade 1	C	F	66	54	1.93	0
T3-06	Meningioma, unspecified	I	F	62	50.4	1.8	3
T0-07	Meningioma, WHO Grade 1	C	M	60	50.4	1.8	0
T0-08	Meningioma, WHO Grade 1	C	M	73	50.4	1.8	0

Abbreviations * C: control case; I: Index case ** Prescribed dose

was defined as dose to water. From MC calculations we also retrieved dose-averaged linear energy transfer (LET_d) distributions, in order to investigate if optic apparatus structures have been located in an elevated LET_d region. In the LET_d calculation secondary electrons, secondary protons, deuterons, and alphas are taken into account. For each voxel a dose weighted average of the energy loss divided by length travelled by particles is scored [17]. As the highest LET areas may appear at a considerable distance from the primary treatment volume in areas, where little dose is delivered, additionally RBE dose distributions according to McNamara variable RBE model [18], were calculated. For optic apparatus structures α/β ratio of 2 was considered.

Each of the analysed treatment plans was delivered on a ProBeam Connect (Varian Medical systems, Palo Alto, USA) proton therapy system in a dry run, to obtain treatment delivery log files. The log files were used to obtain the delivery time of a spot. The readouts in the log files are affected by uncertainty. The only information obtained from the log files in this study was spot duration. Due to the nature of the pencil beam scanning technique, measuring time structure on the spot-by-spot level is unpractical, therefore we rely on the delivery log files. Spot timing in the log files is recorded with a time resolution of up to 1 μs. The typical spot duration is in the order of several ms. Spot duration in a particular delivery can be affected by day-to-day variations in the setup of the delivery equipment (e.g., cyclotron). Furthermore, interlocks during a delivery of the field can introduce variations in spot durations after resumption of the field.

Such scenarios were not considered in the current study, as all spot-wise dose rates were calculated based on a log file from a single uninterrupted dry-run delivery. 3 fields were delivered multiple times to obtain insights in reproducibility of spot durations in uninterrupted deliveries. Variation is spot duration was found to be 0.1±0.9%.

The dose rate per voxel for every spot in the plan was defined as a ratio between dose in the voxel and the delivery time of the spot. The dose and dose rate distributions per spot were used to define and explore various dose and dose rate-related metrics, with a focus on the maximum voxel-wise dose rate (MDR) metric.

MDR is defined on the treatment plan basis and is calculated as the maximum dose rate as seen by a voxel considering all dose rate contributions to the individual spots.

Once the MDR distribution for a plan is defined, based on this distribution, near-maximum (MDR2) dose rates were calculated for the structures which are involved in the optic apparatus: optic chiasm (OC), optic nerve left (ONL) and right (ONR). MDR2 can be considered analogous to the DVH metric D2. MDR2 is near-maximum MDR delivered to 2% of the volume of the structure-of-interest.

Results

Figure 1 demonstrates D2 delivered to the associated structures of the optical apparatus: optic chiasm (OC), left and right optic nerve (ONL, ONR). The optical apparatus of the two toxicity index cases (T4-03 and T3-06)
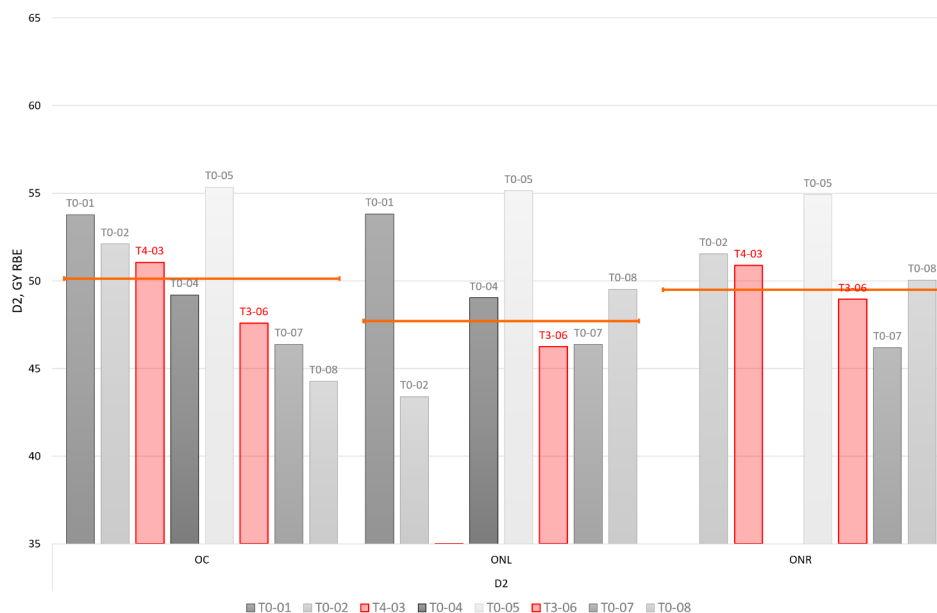

Fig. 1 D2 metrics of the optic apparatus structures for the studied patient group. Toxicity index cases are indicated in red. Orange line indicates median D2 value per each considered structure: optic chiasm (OC), optic nerve left and right (ONL, ONR)
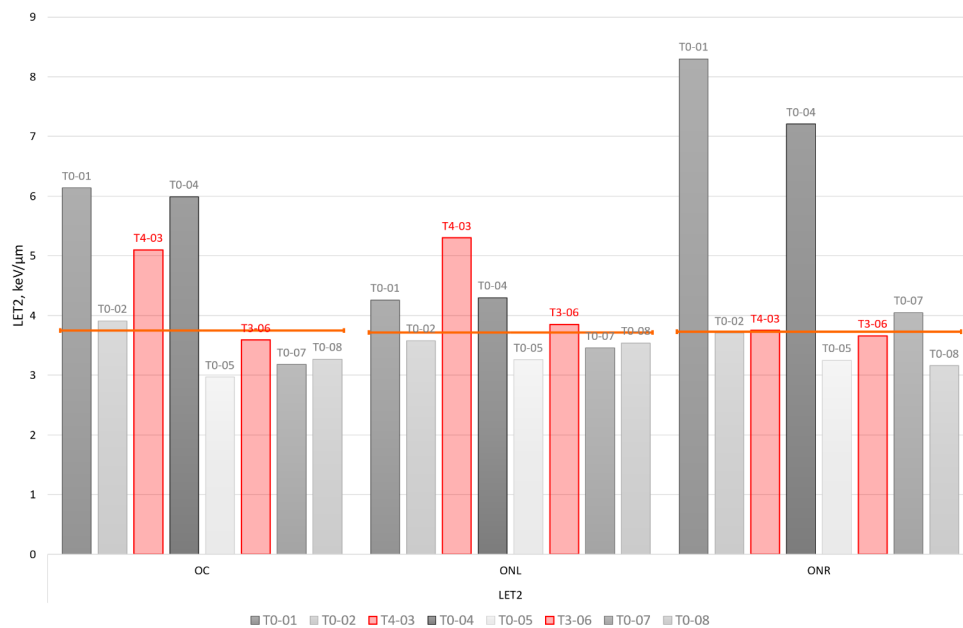
Fig. 2 shows near-maximum LET values for the 2 index and 6 control cases analysed in this study. Near-maximum LET is determined as LET delivered to 2% of the volume of the OAR

was not exposed to an unusually high dose level (D2) compared to other similar intracranial cases.

Therefore, a toxicity explanation linked solely to dose-volume effects seems unlikely for these two index cases. For cases T4-03 and T3-06 complications developed in the left pre-chiasmatic optic nerve. In both cases, the section with RION, as visible on the follow up MRI, was part of the structure "optic chiasm" in the planning structure set (in accordance with the contouring guidelines).

Figure 2. LET2 metrics of the optical apparatus structures for the studied patient group. Toxicity index cases are indicated in red. Orange line indicates median LET2 value per each considered structure: optic chiasm (OC), optic nerve left and right (ONL, ONR).

The plot shows the highest LET2 for the three structures of the optic apparatus. Similarly, as with dose metrics D2, the toxicity cases do not show unusually high near-maximum LET values in the structures of the optical apparatus. RION, as identified on the follow up MRI, was overlapping with the structure "optic chiasm" in the planning structure set.

Figure 3 shows D2 metrics based on dose distributions as calculated using variable RBE model proposed by McNamara. Although the dose values should be interpreted with caution, since variable RBE models impose considerable uncertainty due to lack of in vivo validation, the approach allows for relative comparison of various treatment plans and their dose contribution to organs at risk.

Voxel-wise maximum dose rates (MDR) in the optical apparatus of the 2 index and 6 control cases are shown in

Fig. 4. Similarly, as before, the plot shows the maximum MDR as seen by 2% of the volume of any of the three structures in the optical apparatus: OC, ONL, ONR.

The optic chiasm of the two toxicity cases (T4-03 and T3-06), which could not be explained by high D2 values, appears to be exposed to a higher MDR2 than the optic chiasm of the non-toxicity cases. The high MDR2 values observed in both cases can be attributed to a single field from the treatment plans. As a result, we investigated whether the delivery of such high MDR2 values from a field to an optical structure is unusual within our dataset. Figure 5 shows a box plot of near-maximum MDR2 per field per optical structure. The box plot is constructed of 84 data points, which corresponds to 28 fields (3 to 4 fields per plan) × 3 OARs (OC, ONL, ONR).

The highest data points are associated with the two unexplained toxicity cases: T3-06 and T4-03. This suggests that the exposure of the optical structures to such high dose rates is atypical.

Figure 6 demonstrates MDR maps of the two fields delivering relatively high dose rates to the OC and ONL (case T3-06) and OC (T4-03) overlayed on the planning CTs of the patients

The area, where the high dose rate cloud is overlapping with the structures of the optical apparatus, correlates well with the area of the developed toxicity, as could be identified on MR images.
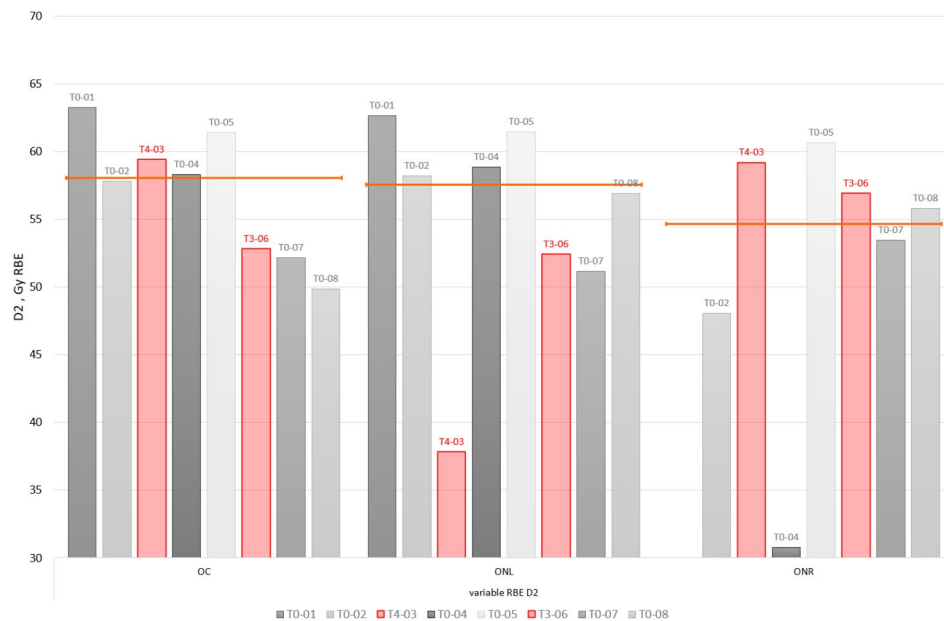
Fig. 3 D2 metrics (as per variable RBE model by McNamara) of the optic apparatus structures for the studied patient group. Toxicity index cases are indicated in red. Orange line indicates median D2 value per each considered structure: optic chiasm (OC), optic nerve left and right (ONL, ONR)
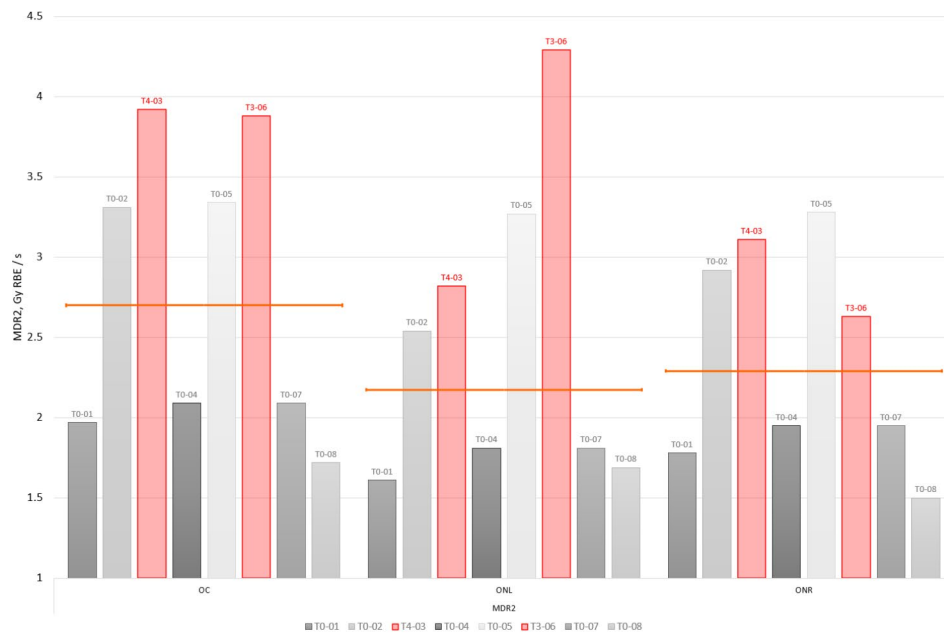

Fig. 4 Voxel wise maximum dose rate metrics (MDR2) of the optic apparatus structures for the analysed patient group. Toxicity index cases are indicated in red. Orange line indicates median MDR2 value per each considered structure: optic chiasm (OC), optic nerve left and right (ONL, ONR)

Discussion

The analysed patient group consists of 2 index toxicity and 6 similar non-toxicity control cases. The non-toxicity cases were matched by the proximity of the target volume to optical structures as well as the indication for treatment. The patients were similarly treated on PSI Gantry 3 (ProBeam Connect) in a time period between October 2019 and February 2022.

A dose metric D2 above a threshold dose (above 60 Gy_{RBE}) [19] increases the risk for development of late optic pathway toxicities. However, it can also be seen that the two toxicity index cases were associated with considerably lower D2 dose levels: 51.05 Gy_{RBE} and 48.95 Gy_{RBE} for the cases T4-03 and T3-06, respectively (Fig. 1). Although significant variability in terms of sensitivity to dose exists in the population, our data suggests
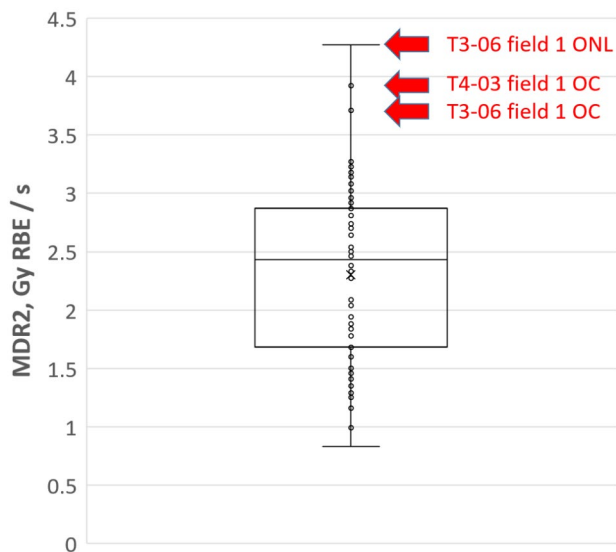
Fig. 5 Box plot of field-wise voxel-wise maximum dose rates (MDR2) to any of the optic apparatus structures: optic chiasm (OC), left and right optic nerves (ONL and ONR). Toxicity index cases, which remain unexplained by dose metrics D2, are indicated in red. MDR2 to OC and ONL for the two index cases correspond to the highest values in the dataset

the existence of other dose promoting adverse effects. LET is widely considered to be an adverse effect promotor, where essentially elevated LET results in an elevated RBE [20]. LET distributions for the given patient group were calculated. However, similarly as with the dose metrics D2, we did not observe a correlation between elevated LET and the location of radiographic injury in the optic apparatus for the index cases, or a variance in LET between index and control cases to suggest an association with optic apparatus injury (Fig. 2). LET on its own is a parameter that is difficult to interpret in terms of association with increased clinical toxicity risk [21–23]. Numerous studies have demonstrated a lack of association between LET and radiation-induced toxicity while other series have suggested a causal relation [24].

Dose rate in proton pencil beam scanning is a parameter that can be considered from various perspectives: instantaneous, averaged over the duration of the delivery of a field or averaged over a predefined period of time (for example, 100 ms) [14]. Furthermore, when calculating dose rate, the considered dose level can be factored in (for example, dose rate is considered only for delivered dose in the voxel above 50 cGy level). We derived a global voxel wise maximum dose rate as a parameter (MDR) to gain initial insights into the dose rate related parameters in the context of the development of late toxicities. MDR is related to a maximum instantaneous dose rate that a voxel has been exposed to disregarding the amount of dose delivered at this dose rate. Nevertheless, we observed that for the two toxicity cases T4-03 and

T3-06, which were difficult to explain in the context of dose metrics, MDR was shown to be elevated compared to other cases in the group (Fig. 4). In fact, MDR2 as high as 3.9 Gy_{RBE}/s and 4.3 Gy_{RBE}/s was observed only for the two unexplained toxicity index cases (T4-03 and T3-06). These high MDR values could be traced back to a contribution from a single field in the plan for both cases. Figure 5 has shown that such high dose rates delivered from a field to structures of the optical apparatus are atypical.

In this study we demonstrate the relative differences in MDR between index and control cases. A word of caution should be mentioned with regards to broader adoption of absolute scale. The MDR metric is sensitive to dose threshold value, which in the current study was set to 1 cGy per fraction. By adopting different parametrization, the obtained absolute MDR values may vary considerably. The choice of the dose threshold value in MDR calculations is a subject of further studies.

For the two individual fields contributing to the high MDR values for the cases T4-03 and T3-06 we calculated field-wise MDR distributions and overlayed them with the delineated CT, as shown in Fig. 6. The high MDR regions intersect remarkably well with the damaged left pre-chiasmatic optic nerve structure, which, for both cases, was associated with the late optic toxicity that was identifiable based on follow-up MR images.

To put the observations in the context to the FLASH effect it should be highlighted that, the dose rates for the clinical cases in this study are well below FLASH dose rates, which are currently considered to be above 40 Gy/s. Furthermore, a FLASH effect is achieved at high dose levels. On the contrary to that, we observe low dose levels delivered at high dose rates. For both index cases the dose delivered at 3.5 Gy/s or more was less than 10% of total dose delivered to the toxicity area. Finally, at this point overwhelming majority of FLASH effect demonstrations are related to acute toxicities, while RION, which is considered in the current study, is late toxicity.

When discussing relative biological effectiveness (RBE), there are numerous parameters that define its characteristics [25]. Synergic effects between dose rate and LET could be explored further and might reveal a better predictive model for late toxicity development. In our investigated cases regions of high LET and regions of high dose rate spatially do not correlate. High dose rates can for example also occur on the proximal edge of a field, where the LET is usually low. If a significant dose-enhancing effect linked to dose rate exists, it is probable that predicting the risk of toxicity would be more accurate by considering the cumulative dose delivered at or above a specific dose rate threshold, rather than solely relying on the instantaneous maximum dose rate. We are further exploring the dose above dose rate parameter
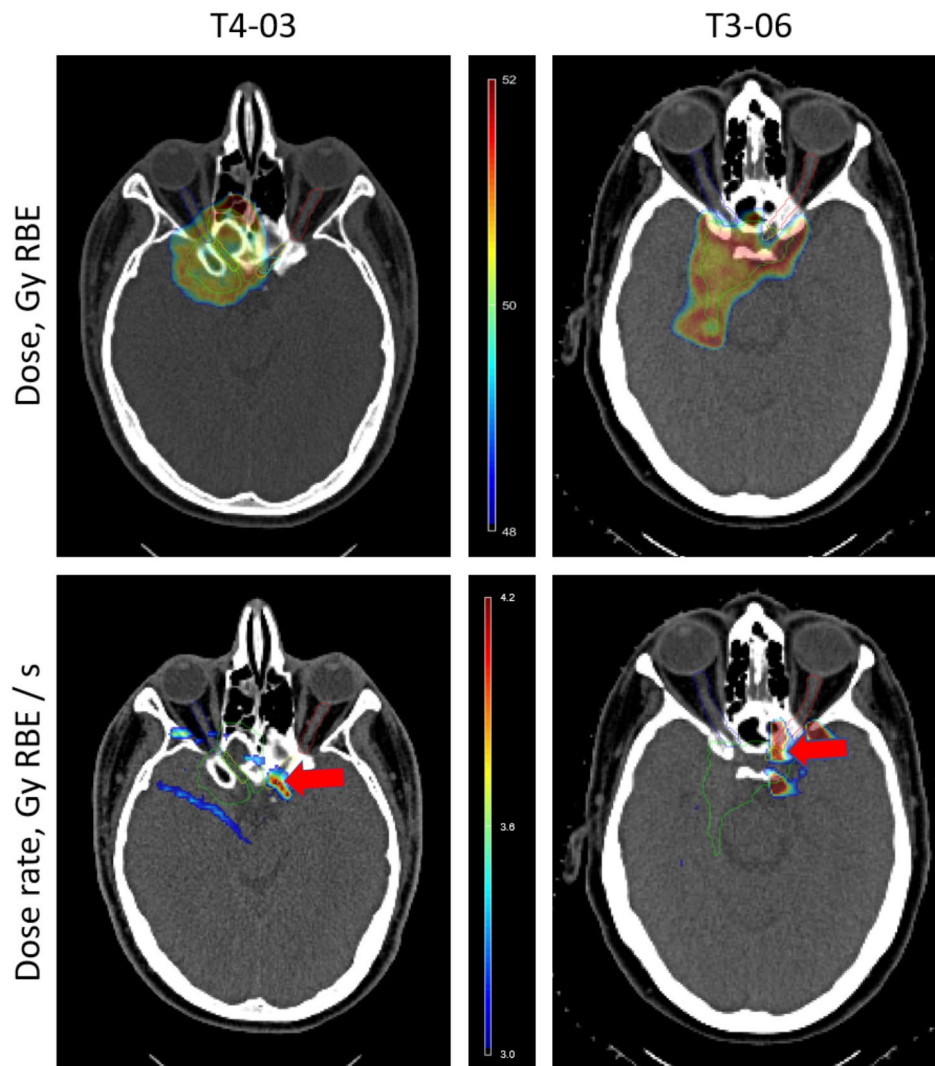
Fig. 6 Overlay of dose and voxel wise maximum dose rate (MDR) distributions on CT images of the two toxicity cases (T4-03 and T3-06). Dose rate distributions are shown for the fields contributing the highest MDR values. The maximum dose rate distribution above 3 Gy$_{RBE}$/s threshold is shown. High dose rate areas overlap with pre-chiasmatic left optic nerve areas, which developed radiation induced optic neuropathy (RION) on the follow-up MR images. The optic chiasm is shown in yellow, left and right optic nerves are shown in red and blue, respectively, CTV is shown in green, and area of RION is indicated with a red arrow. The dose and dose-rate colourwashes are displayed at the centre of the Figure

space in combination with dose delivered at an elevated RBE due to LET.

The strong limitation of this study is the size of the data set. Fortunately, the incidence of optic apparatus toxicities is low in our patients with intracranial disease [11, 12]. Therefore, the possibility to acquire a sufficiently large data set to prove or disprove the hypothesis will require a multi-institutional collaboration, similar as suggested in the European Particle Therapy Toxicity Workshop (Leuven, Belgium, 04.10.2022). Nevertheless, dose rate calculation for conventional proton treatment plans currently is not a feature readily available in commercial treatment planning systems (TPS). Such calculations require in-house developments or dedicated research builds of TPS.

Eventually, other clinical factors may have influenced the development of the toxicity. For instance, one out of two toxicity cases is a patient more than 60 years old.

In conclusion, our observations reveal large variations in instantaneous dose rates experienced by different volumes within our patient cohort, even when considering the same indications and beam arrangement. Furthermore, we observed an overlap between high-dose rate areas and regions of developed optic toxicities as identified on MR images. At this point, it is not feasible to establish causality between exposure to high dose rates and the development of late optic apparatus toxicities due to the low incidence of injury. Since the number of toxicity cases per institute is generally low, a multi-institutional study would be necessary to provide evidence for

the correlation between elevated dose rate and the radiation injury. Further radiobiology studies investigating the effects of low/high dose rate proton exposures will hopefully provide additional insights and further elucidate this potential radiobiological impact.

Abbreviations

CTCAE	Common Terminology Criteria for Adverse Events
DR	Dose rate
LET	Linear energy transfer
LET_d	Dose-averaged linear energy transfer
MC	Monte Carlo
MD	Medical doctor
MDR	Voxel-wise maximum dose rate
OAR	Organ at risk
OC	Optic chiasm
ONL	Optic nerve left
ONR	Optic nerve right
RBE	Relative biological effectiveness
RION	Radiation induced optic neuropathy
TPS	Treatment planning system

Author contributions
Arturs Meijers: Conceptualization, Methodology, Software, Formal analysis, Investigation, Writing - Original Draft, Visualization, Juliane Daartz: Conceptualization, Writing - Review & Editing, Antje-Christin Knopf: Conceptualization, Writing - Review & Editing, Michelle van Heerden: Writing - Review & Editing, Nicola Bizzocchi: Writing - Review & Editing, Miriam Vazquez Varela: Writing - Review & Editing, Data Curation, Barbara Bachtiary: Writing - Review & Editing, Data Curation, Alessia Pica: Writing - Review & Editing, Data Curation, Helen A Shih: Writing - Review & Editing, Supervision, Damien Charles Weber: Conceptualization, Writing - Review & Editing, Supervision.

Data availability
No datasets were generated or analysed during the current study.

Declarations

Ethical approval and consent to participate
Not Applicable.

Consent for publication
Not Applicable.

Competing interests
Arturs Meijers is a Clinical Advisory Committee member of Ion Beam Applications Helen A Shih is a Clinical Advisory Committee member of Ion Beam Applications Helen A Shih has received P01 funding to better understand proton therapy as a payment to the institution.

Author details
[1]Center for Proton Therapy, Paul Scherrer Institut, Forschungsstrasse 111, Villigen 5232, Switzerland
[2]Department of Radiation Oncology, Massachusetts General Hospital, Harvard Medical School, Boston, MA, USA
[3]Institute for Medical Engineering and Medical Informatics, School of Life Science FHNW, Muttenz, Switzerland
[4]Department of Radiotherapy and Radiation Oncology, Faculty of Medicine, University Hospital Carl Gustav Carus, Technische Universität Dresden, Dresden, Germany
[5]Department of Radiation Oncology, Massachusetts General Hospital, Boston, MA, USA
[6]Department of Radiation Oncology, University Hospital of Zürich, Zürich, Switzerland
[7]Department of Radiation Oncology, Inselspital, Bern University Hospital, University of Bern, Bern, Switzerland

References
1. Mohan RA. Review of Proton Therapy - current status and future directions. Precis Radiat Oncol. 2022;6(2):164–76. https://doi.org/10.1002/pro6.1149. Epub 2022 Apr 27. PMID: 36160180; PMCID: PMC9499036.
2. Pedroni E, Böhringer T, Coray A, Egger E, Grossmann M, Lin S, Lomax A, Goitein G, Roser W, Schaffner B. Initial experience of using an active beam delivery technique at PSI. Strahlenther Onkol. 1999;175 Suppl 2:18–20. https://doi.org/10.1007/BF03038879. PMID: 10394388.
3. Paganetti H, Beltran C, Both S, Dong L, Flanz J, Furutani K, Grassberger C, Grosshans DR, Knopf AC, Langendijk JA, Nystrom H, Parodi K, Raaymakers BW, Richter C, Sawakuchi GO, Schippers M, Shaitelman SF, Teo BKK, Unkelbach J, Wohlfahrt P, Lomax T. Roadmap: proton therapy physics and biology. Phys Med Biol. 2021;66(5). https://doi.org/10.1088/1361-6560/abcd16. PMID: 33227715; PMCID: PMC9275016.
4. Ling CC, Gerweck LE, Zaider M, Yorke E. Dose-rate effects in external beam radiotherapy redux. Radiother Oncol. 2010;95(3):261-8. https://doi.org/10.1016/j.radonc.2010.03.014. Epub 2010 Apr 1. PMID: 20363041.
5. Dale RG. Dose-rate effects in targeted radiotherapy. Phys Med Biol. 1996;41(10):1871-84. https://doi.org/10.1088/0031-9155/41/10/001. PMID: 8912367.
6. Beddok A, Lahaye C, Calugaru V, De Marzi L, Fouillade C, Salvador S, Font-bonne JM, Favaudon V, Thariat J. A comprehensive analysis of the Relation-ship between Dose Rate and Biological effects in Preclinical and Clinical studies, from brachytherapy to flattening Filter Free Radiation Therapy and FLASH Irradiation. Int J Radiat Oncol Biol Phys. 2022;113(5):985–95. Epub 2022 Feb 26. PMID: 35227789.
7. Ben Kacem M, Benadjaoud MA, Dos Santos M, Soysouvanh F, Buard V, Tarlet G, Le Guen B, François A, Guipaud O, Milliat F, Paget V. Variation of 4 MV X-ray dose rate strongly impacts biological response both in vitro and in vivo. Sci Rep. 2020;10(1):7021. https://doi.org/10.1038/s41598-020-64067-4. PMID: 32341396; PMCID: PMC7184727.
8. Kann BH, Yu JB, Stahl JM, Bond JE, Loiselle C, Chiang VL, Bindra RS, Gerrard JL, Carlson DJ. The impact of cobalt-60 source age on biologically effective dose in high-dose functional Gamma Knife radiosurgery. J Neurosurg. 2016;125(Suppl 1):154–159. https://doi.org/10.3171/2016.6.GKS161497. PMID: 27903196.
9. Wozny AS, Alphonse G, Battiston-Montagne P, Simonet S, Poncet D, Testa E, Guy JB, Rancoule C, Magné N, Beuve M, Rodriguez-Lafrasse C. Influence of Dose Rate on the Cellular Response to Low- and High-LET Radiations. Front Oncol. 2016;6:58. https://doi.org/10.3389/fonc.2016.00058. Erratum in: Front Oncol. 2017;6:271. PMID: 27014633; PMCID: PMC4790194.
10. Ben Kacem M, Benadjaoud MA, Dos Santos M, Buard V, Tarlet G, Le Guen B, François A, Guipaud O, Milliat F, Paget V. Variation of 4 MV X-ray dose rate in fractionated irradiation strongly impacts biological endo-thelial cell response in vitro. Int J Radiat Biol. 2022;98(1):50–59. doi: 10.1080/09553002.2022.1998703. Epub 2021 Nov 3. PMID: 34705615.
11. Köthe A, Feuvret L, Weber DC, Safai S, Lomax AJ, Fattori G. Assessment of Radiation-Induced Optic Neuropathy in a multi-institutional cohort of Chor-doma and Chondrosarcoma patients treated with Proton Therapy. Cancers (Basel). 2021;13(21):5327. https://doi.org/10.3390/cancers13215327. PMID: 34771490; PMCID: PMC8582447.
12. Kountouri M, Pica A, Walser M, Albertini F, Bolsi A, Kliebsch U, Bachtiary B, Combescure C, Lomax AJ, Schneider R, Weber DC. Radiation-induced optic neuropathy after pencil beam scanning proton therapy for skull-base and head and neck tumours. Br J Radiol. 2020;93(1107):20190028. https://doi.org/10.1259/bjr.20190028. Epub 2019 Aug 1. PMID: 31322969; PMCID: PMC7066972.
13. Eulitz J, Troost GC, Klünder E, Raschke L, Hahn F, Schulz C, Seidlitz E, Thiem A, Karpowitz J, Hahlbohm C, Grey P, Engellandt A, Löck K, Krause S, Lühr M. Increased relative biological effectiveness and periventricular radiosensitivity

in proton therapy of glioma patients. Radiother Oncol. 2023;178:109422. Epub 2022 Nov 23. PMID: 36435337.

14. Daartz J, Madden T, Lalonde A, Cascio E, Verburg JM, Shih H, MacDonald S, Hachadorian R, Schuemann J. Voxel-wise dose rate calculation in clinical pencil beam scanning proton therapy. Phys Med Biol. 2024 Feb 7. https://doi.org/10.1088/1361-6560/ad2713. Epub ahead of print. PMID: 38324902.

15. Danesh-Meyer HV. Radiation-induced optic neuropathy. J Clin Neurosci. 2008;15(2):95–100. https://doi.org/10.1016/j.jocn.2007.09.004. PMID: 18068989.

16. Souris K, Lee JA, Sterpin E. Fast multipurpose Monte Carlo simulation for proton therapy using multi- and many-core CPU architectures. Med Phys. 2016;43(4):1700. https://doi.org/10.1118/1.4943377. PMID: 27036568.

17. Wagenaar D, Tran LT, Meijers A, Marmitt GG, Souris K, Bolst D, James B, Biasi G, Povoli M, Kok A, Traneus E, van Goethem MJ, Langendijk JA, Rosenfeld AB, Both S. Validation of linear energy transfer computed in a Monte Carlo dose engine of a commercial treatment planning system. Phys Med Biol. 2020;65(2):025006. https://doi.org/10.1088/1361-6560/ab5e97. PMID: 31801119.

18. McNamara AL, Willers H, Paganetti H. Modelling variable proton relative biological effectiveness for treatment planning. Br J Radiol. 2020;93(1107):20190334. https://doi.org/10.1259/bjr.20190334. Epub 2019 Nov 18. PMID: 31738081; PMCID: PMC7066955.

19. Ataídes FabrícioG, et al. Radiation-Induced Optic Neuropathy: Literature Review. Neuro-ophthalmology (Aeolus Press). 4 Nov. 2020;45:3 172–80. https://doi.org/10.1080/01658107.2020.1817946.

20. McMahon SJ, Paganetti H, Prise KM. LET-weighted doses effectively reduce biological variability in proton radiotherapy planning. Phys Med Biol. 2018;63(22):225009. https://doi.org/10.1088/1361-6560/aae8a5. PMID: 30412471.

21. Mohan R, Peeler CR, Guan F, Bronk L, Cao W, Grosshans DR. Radiobiological issues in proton therapy. Acta Oncol. 2017;56(11):1367–1373. https://doi.org/10.1080/0284186X.2017.1348621. Epub 2017 Aug 22. Erratum in: Acta Oncol. 2019;58(1):132. PMID: 28826292; PMCID: PMC5842809.

22. Vaniqui A, Vaassen F, Di Perri D, Eekers D, Compter I, Rinaldi I, van Elmpt W, Unipan M. Linear Energy Transfer and relative Biological Effectiveness Investigation of various structures for a cohort of Proton patients with brain tumors. Adv Radiat Oncol. 2022;8(2):101128. https://doi.org/10.1016/j.adro.2022.101128. PMID: 36632089; PMCID: PMC9827037.

23. Wagenaar D, Schuit E, van der Schaaf A, Langendijk JA, Both S. Can the mean linear energy transfer of organs be directly related to patient toxicities for current head and neck cancer intensity-modulated proton therapy practice? Radiother Oncol. 2021;165:159–65. Epub 2021 Sep 14. PMID: 34534614.

24. Bolsi A, Placidi L, Pica A, Ahlhelm FJ, Walser M, Lomax AJ, Weber DC. Pencil beam scanning proton therapy for the treatment of craniopharyngioma complicated with radiation-induced cerebral vasculopathies: A dosimetric and linear energy transfer (LET) evaluation. Radiother Oncol. 2020;149:197–204. doi: 10.1016/j.radonc.2020.04.052. Epub 2020 May 5. PMID: 32387488.

25. Underwood TSA, McNamara AL, Appelt A, Haviland JS, Sørensen BS, Troost EGC. A systematic review of clinical studies on variable proton relative biological effectiveness (RBE). Radiother Oncol. 2022;175:79–92. Epub 2022 Aug 18. PMID: 35988776.

Publisher's Note